Article

Experimental evidence for the functional relevance of anion–π interactions

DAWSON, Ryan E., *et al*.

Abstract

Attractive in theory and confirmed to exist, anion–π interactions have never really been seen at work. To catch them in action, we prepared a collection of monomeric, cyclic and rod-shaped naphthalenediimide transporters. Their ability to exert anion–π interactions was demonstrated by electrospray tandem mass spectrometry in combination with theoretical calculations. To relate this structural evidence to transport activity in bilayer membranes, affinity and selectivity sequences were recorded. π-acidification and active-site decrowding increased binding, transport and chloride > bromide > iodide selectivity, and supramolecular organization inverted acetate > nitrate to nitrate > acetate selectivity. We conclude that anion–π interactions on monomeric surfaces are ideal for chloride recognition, whereas their supramolecular enhancement by π,π-interactions appears perfect to target nitrate. Chloride transporters are relevant to treat channelopathies, and nitrate sensors to monitor cellular signaling and cardiovascular diseases. A big impact on organocatalysis can be expected from the stabilization of anionic [...]

Reference

DAWSON, Ryan E., *et al*. Experimental evidence for the functional relevance of anion–π interactions. *Nature chemistry*, 2010, vol. 2, no. 7, p. 533-538

DOI : 10.1038/nchem.657

Experimental evidence for the functional relevance of anion-π interactions

Ryan E. Dawson,[1,5] Andreas Hennig,[1,5] Dominik P. Weimann,[2] Daniel Emery,[1] Velayutham Ravikumar,[1] Javier Montenegro,[1] Toshihide Takeuchi,[1] Sandro Gabutti,[3] Marcel Mayor,[3,4] Jiri Mareda,[1] Christoph A. Schalley[2] & Stefan Matile[1]*

[1]Department of Organic Chemistry, University of Geneva, Geneva, Switzerland. [2]Institut für Chemie und Biochemie der Freien Universität, Berlin, Germany. [3]Department of Chemistry, University of Basel, Basel, Switzerland. [4]Institute of Nanotechnology, Karlsruhe Institute of Technology, Germany. [5]These two authors contributed equally to the study. *e-mail: stefan.matile@unige.ch.

Attractive in theory and confirmed to exist, anion-π interactions have never really been seen at work. To catch them in action, we prepared a collection of monomeric, cyclic and rod-shaped naphthalenediimide transporters. Their ability to exert anion-π interactions was demonstrated by electrospray tandem mass spectrometry in combination with theoretical calculations. To relate this structural evidence to transport activity in bilayer membranes, affinity and selectivity sequences were recorded. π–Acidification and active-site decrowding increased binding, transport and chloride > bromide > iodide selectivity, supramolecular organization inverted acetate > nitrate to nitrate > acetate selectivity. We conclude that anion-π interactions on monomeric surfaces are ideal for chloride recognition, whereas their supramolecular enhancement by π,π-interactions appears perfect to target nitrate. Chloride transporters are relevant to treat channelopathies, nitrate sensors to monitor cellular signaling and cardiovascular diseases. Big impact on organocatalysis is expected from the stabilization of anionic transition-states on chiral π-acidic surfaces.

Anion-π interactions take place between anions and π-acidic aromatic surfaces with positive quadrupole moments[1-11]. They complement cation-π interactions between cations and π-basic aromatic surfaces with the inverted, negative quadrupole moments[12]. The experimentally observed contacts between π-acidic aromatic rings and anions are the non-covalent anion-π interaction, the strongly covalent or Meisenheimer complex, the weakly covalent or charge-transfer interaction, and the C-H···X$^-$ hydrogen bond[10]. Contrary to the ubiquitous cation-π interactions, π-acidic aromatic surfaces and their interaction with anions are relatively rare and hard to access[11]. It is in part for this reason that the functional relevance of anion-π interactions remains to be shown.

Recently, some of us reported functional significance for anion-π interactions in the context of anion transport across lipid bilayer membranes[13,14]. Important with regard to basic science as well as applications in organic, biological, medicinal and materials chemistry, anion recognition and transport is otherwise achieved today in elegant compositions of ion pairing, hydrogen bonding and, very recently, also anion-macrodipole interactions[15-20]. To use anion-π interactions for transport, three naphthalenediimides (NDIs)[21-25] were lined up in rigid-rod oligomer (O-NDI) **1** (Fig. 1). The obtained π-slide was thought to be long enough to span a lipid bilayer membrane and allow anions to move along the π-acidic surfaces (Fig. 1). However, whereas excellent activity and anion selectivity were found, it was not possible to prove experimentally that anion-π interactions really exist that account for functional behavior, or, at best, the acquired evidence is indirect. For example, contributions from amides or potentially charged peptide chains at both termini of the slides to anion binding and transport could never be fully ruled out[13,14]. Herein, unequivocal, clear-cut experimental evidence for the functional relevance of anion-π interactions is presented.

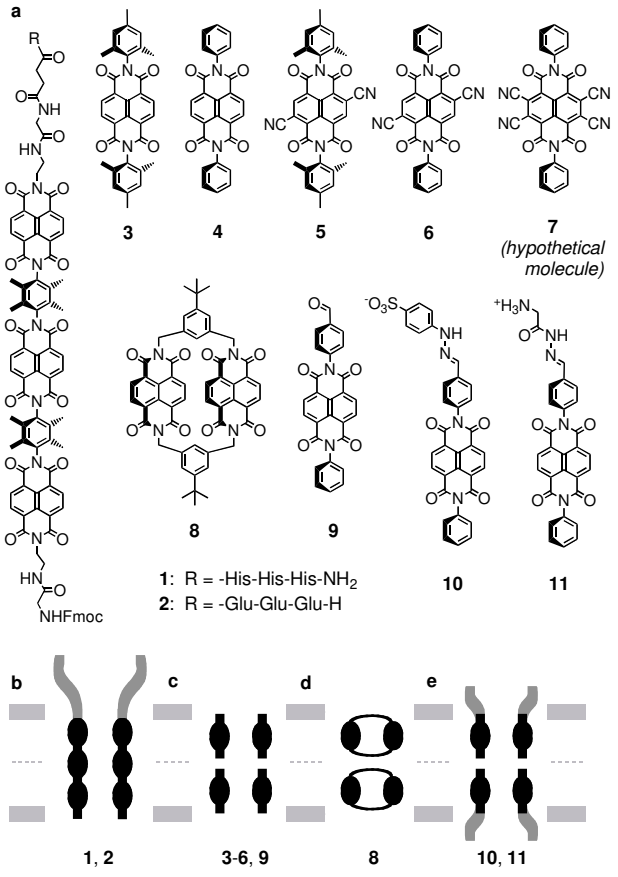

Figure 1 | Structures and hypothesized active suprastructures of anion-π transporters. NDIs **1**-**11** (**a**) are thought to possibly self-assemble into transmembrane dimers of single-leaflet bundles (**c**) that are stabilized by hydrophilic heads (**b**, **e**) and vertical (**b**) or horizontal (**d**) crosslinking.

Results

Design. To study anion-π interactions at work, we designed and synthesized, as far as possible, monomeric, macrocyclic and rod-shaped O-/NDIs **2**-**11**, where anion-π interactions are systematically modulated and interferences from unrelated effects vigorously excluded (Fig. 1a). The original amphiphile **1** is composed of a transmembrane O-NDI tail for transport by anion-π interactions and a trihistidine head for delivery to the membrane (Fig. 1b)[13]. In amphiphile **2**, the cationic trihistidine is replaced by an anionic triglutamate to determine the contributions from the peptide head to anion selectivity.

Deconstructing rods **1** and **2** to extract anion-π interactions in purest possible form, the minimalist NDI **3** was defined as the ideal starting point. The *ortho*-methyl groups of the peripheral mesitylenes point into the anion-π binding site on the pyridinedione surface and thus contribute to active-site confinement and C-H···anion bonding. Moreover, they should obstruct intermolecular π,π-interactions and thus interfere with self-organization into supramolecular architectures. From there, active-site decrowding and π-acidity are systematically maximized by *o*-methyl removal in **4** and **6** and addition of cyano acceptors in the core of **5** and **6**. In dicyano NDIs, the LUMO (lowest unoccupied molecular orbital) drops from -4.0 to -4.2 eV[22] and the quadrupole moment increases from $Q_{zz} \approx$ +20 to $Q_{zz} \approx$ +39 B[13], four cyano groups give $Q_{zz} \approx$ +56 B[13]. For comparison, hexafluorobenzene has Q_{zz} = +9.5 B, trinitrotoluene (TNT) $Q_{zz} \approx$ +20 B[1].

Active suprastructures in lipid bilayer membranes are intrinsically complex and dynamic, usually thermodynamically unstable[20,26], and include not only NDI-anion but also NDI-lipid and NDI-NDI interactions (Fig. 1). As simplified working hypothesis, NDI monomers were assumed to align along the lipid tails in one leaflet. Preferred NDI-NDI over NDI-lipid interactions gives single-leaflet NDI bundles, which could further dimerize into transmembrane dimers (Fig. 1c). From there, we explore the impact of vertical crosslinking (Fig. 1b), horizontal crosslinking[24] (Fig. 1d), hydrophilic anchoring[13] (Fig. 1b/e), π-acidification and peripheral decrowding on the self-organization of the active transmembrane dimers.

Synthesis. The synthesis of most target molecules was accomplished based on or in analogy to reported procedures (figs. S1-S3)[27]. The synthesis of NDIs with cyano groups in the core required special attention (Fig. 2). Routine bromination of naphthalene dianhydride (NDA) with dibromoisocyanuric acid followed by reaction of crude **12** with **13** gave NDI **14**, and nucleophilic substitution with CuCN gave **5**. This approach to dicyano NDIs was not applicable to NDI **6**. The problem was that with the more reactive aniline, core substitution of NDA **12** coincided with diimide formation, and all attempts to establish chemoselectivity failed. However, results from anion transport with **3**-**5** suggested that NDI **6** would have perfect properties. These expectations justified an in-depth search of new approaches to **6**. Best results were obtained when NDA **12** was reacted first with ammonium acetate under acidic conditions to prevent core substitution. The primary diimide **15** was then reacted with CuCN to afford **16**, where the peripheral phenyls could be added by a transition-metal catalyzed C-N coupling with phenyl boronate **17**, and traces of the desired NDI **6** could be extracted and purified from nearly intractable product mixtures.

Both the classical approach to **5** and the alternative approach to **6** were not applicable to the synthesis of tetracyano NDI **7**. This persistent failure in synthesis despite massive industrial interest[25] suggested that tetracyano NDIs may be either too electron deficient to exist or too intractable to be observed.

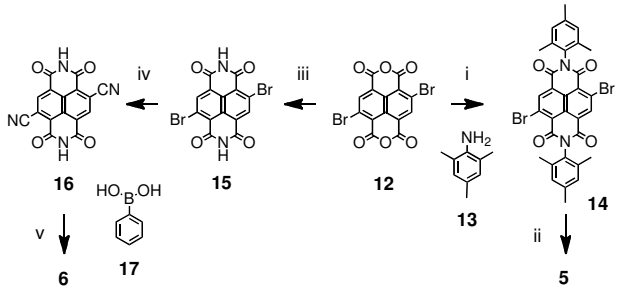

Figure 2 | Synthesis of dicyano NDIs. i) Acetic acid (AcOH), 80 °C, 12 h, >28% (2 steps); ii) CuCN, *N*-methyl-2-pyrrolidinone (NMP), 100 °C, 5 h, 63%; iii) NH_4OAc, AcOH, reflux, 1 h, 77%; iv) CuCN, NMP, 100 °C; v) $Cu(OAc)_2$, triethylamine, dimethylacetamide, 4.2% (2 steps).

ESI-FTICR-MS-MS Experiments. The use of nuclear magnetic resonance (NMR) spectroscopy and isothermal titration calorimetry (ITC) to detect anion-π interactions was not meaningful with NDI monomers because binding is too weak and NMR shifts too small. In this demanding situation, electrospray ionization ion cyclotron resonance tandem mass spectrometry (ESI-FTICR-MS-MS) experiments[28] appeared ideal to deliver the desired direct experimental evidence for anion-π interactions. Mass spectrometry offers the additional advantage that non-solvated complexes are monitored which can more easily be compared to quantum chemical calculations than the corresponding complexes in solution. Furthermore, the gas phase likely resembles more closely the situation in the unpolar core of the lipid bilayers used in the following than the situation in competing polar solvents.

Equimolar solutions of NDIs **3**-**5** and **8** and salts of different anions were electrosprayed from acetonitrile under as mild as possible ionization conditions. Quite fragile NDI-anion complexes of **3**-**5** were observed for Cl^-, Br^- and NO_3^- (fig. S4). With dimer **8**, an additional series of anions was observed to bind. Adduct detectability decreased with $NO_3^- \sim Cl^- \sim Br^-$ (1:1 and 2:1 adducts) > $I^- \sim H_2PO_4^- \sim OTf^- \sim ClO_4^-$ (1:1 adducts) > $OAc^- \sim {}^-BF_4^-$ (weak 1:1 adducts) > $PF_6^- \sim BPh_4^- \sim SO_4^{2-} \sim MnO_4^-$ (not detected, table S1). Although qualitative as long as no ESI response factors are known[28,29], the preference for chloride among halides and nitrate among oxyanions was interesting (see below).

The formation of dimers was used for competition experiments with NDI monomers **3**-**5** and chloride as preferred anion. An equimolar mixture of NDIs **3** and **4** was electrosprayed together with one equivalent of NEt_4Cl, and the corresponding heterodimer **3**+**4**+Cl^- was isolated (Fig. 3a). Fragmentation of heterodimer **3**+**4**+Cl^- was induced by irradiation with a 25 W infrared (IR) laser. After 100 ms irradiation, Cl^- started to appear together with monomeric NDI **4** alone (Fig. 3b). After 200 ms irradiation, the peak for **3**+**4**+Cl^- nearly disappeared and new peak for **3**+Cl^- appeared besides the dominant peak for **4**+Cl^- (Fig. 3c). These observations demonstrated that NDI **4** binds chloride better than NDI **3** (Table 1, entry 1 vs 2). The same tandem ESI experiment revealed that chloride prefers NDI **5** over NDI **4** and NDI **6** over NDI **5** (figs. S6-S7, Table 1, entries 2-4). The

found selectivity sequence **6>5>4>3** demonstrated increasing anion affinity with increasing π-acidity and decrowding of the anion-π binding site (see below). Different to the more qualitative results from routine ESI-MS measurements, intensities found in ESI-FTICR-MS-MS relate to true gas phase experiments and can be used to determine anion affinity sequences quantitatively[29]. These results from ESI-FTICR-MS-MS were thus of highest importance because they provide direct experimental evidence for anion binding to minimalist NDI models that contain not much else to bind to than a π-acidic surface.

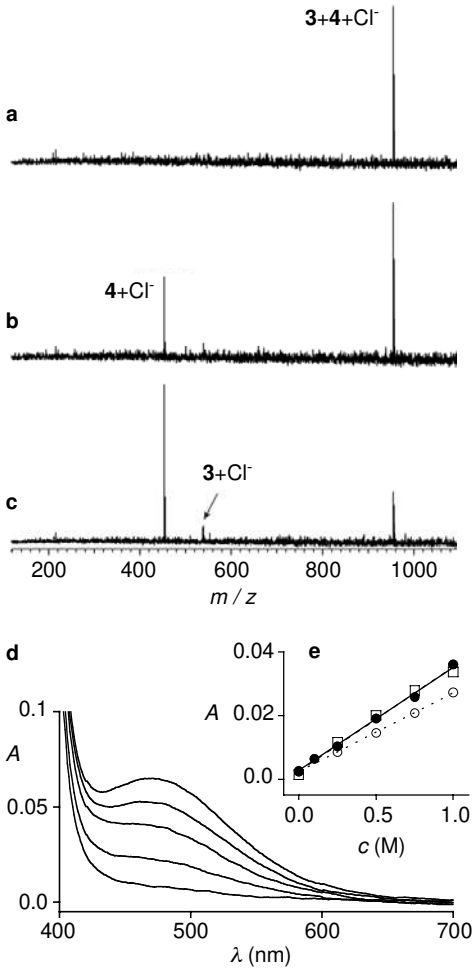

Figure 3 | Laser-induced ESI-MS-MS fragmentation of heterodimer complexes and CT absorption. The spectra show the isolated heterodimer **3+4** with one chloride before (**a**) and after fragmentation induced by a 100 ms (**b**) and a 200 ms laser pulse (**c**). (**d**) Changes in UV/vis absorption of a solution of 300 μM NDI **3** in acetonitrile/chloroform 9:1 in the presence of 0.0, 0.25, 0.5, 0.75 and 1.0 M TBAI (compare **e**○). (**e**) Absorption at the maximum of the CT band as a function of TBAX concentration for 300 μM **3** (○, X = I), 300 μM **4** (●, X = I) and 150 μM **5** (□, 150 μM, X = Br).

Charge-Transfer Complexes. Addition of tetrabutylammonium iodide (TBAI) to NDI **3** in a 9:1 mixture of acetonitrile and chloroform produced an absorption band at 400-650 nm. This transition was assigned to a charge transfer (CT) between the π-acidic NDI and the iodide anion (Fig. 3d). This assignment was supported by a red shift from 470 to 510 nm with decreasing solvent polarity (fig. S9) and a blue-shifted maximum compared to CT with the more easily reducible tetracyanopyrazine[6]. Rose-Drago analysis[6] of the dose response of NDI **3** to TBAI gave a dissociation constant $K_D \approx 5.9$ M (Fig. 3e○, assuming 1:1 stoichiometry[6,27]). Similar results were found for NDI **4** (Fig. 3e●). The red-shifted CT band at $\lambda_{max} \approx$ 520 nm observed with TBABr was in agreement with the high reducibility of dicyano NDI **5** (Fig. 3e□).

Computational Chemistry. Electrostatic potential surfaces were computed at the MP2/6-311++G**//PBE1PBE/6-311G** level as described previously[14]. For NDI **6**, they confirmed that the pyridinedione heterocycles are the regions of highest electron deficiency where anion binding is expected to occur (Fig. 4). Depending on interference from peripheral *o*-methyls or hydrogens, the anion was displaced from the pyridinedione binding site. The weakening of anion-π interactions was reflected in an increasing distance between the NDI plane and anion (R_c distance, Table 1) and only partially compensated by stabilizing C–H•••X$^-$ interactions[14,27]. The N-aryl planes were not perpendicular to the NDI planes, dihedral angles found were between 86° to 62°, a twist that can cause anions to move away from the arene centroid to maximize C–H•••X$^-$ interactions. Their main *ipso-para* axis was occasionally bent out of the NDI plane for the same reason.

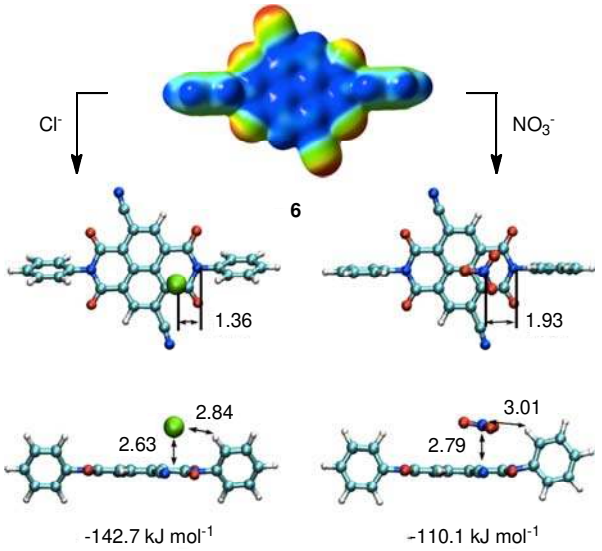

Figure 4 | Molecular modeling of anion-π interactions. Electrostatic potential surface (blue positive, red negative, ±150 kJmol^{-1}, MP2/6-311++G**//PBE1PBE/6-311G**) and DFT (density functional theory) optimized structures of 1:1 chloride and nitrate complexes of NDI **6** (atom color coding, chloride green) with indication of anion location (Å) and interaction energies.

The BSSE-corrected anion binding energies computed at PBE1PBE/6-311++G**//PBE1PBE/6-311G** level[14,30-32] increased with decreasing steric hindrances and increasing π-acidity of the pyridinedione surface (Table 1). For monomeric NDIs, binding energies increased with decreasing distance from the NDI surface and displacement from the pyridinedione binding site. The computed chloride > bromide > nitrate affinity sequences in 1:1 complexes corresponded with results from tandem MS and transmembrane transport. Anion binding by cyclophane **8** was stronger than with monomers **3** and **4** but weaker than with π-acidified monomers **5** and **6**. According to computational results, the properties of tetracyano NDI **7** should further improve those of dicyano NDI **6** with regard to chloride recognition (Table 1, entry 5). However,

Table 1 | Summary of anion binding data for NDIs 2-11 from MS-MS,[a] molecular modeling[b-c] and transmembrane transport.[d-i]

Entry	NDI[j]	Cl^- (MS)[a]	$E_{int}^{Cl^-}$ (kJ/mol)[b]	$E_{int}^{Br^-}$ (kJ/mol)[b]	$E_{int}^{NO_3^-}$ (kJ/mol)[b]	R_e (Å)[c]	Cl^-/I^- [d]	Cl^-/Br^- [e]	NO_3^-/AcO^- [f]	Na^+/K^+ [g]	EC_{50} (HPTS) (μM)[h]	EC_{50} (CF) (μM)[i]
1	**3**	+	-83.3	-72.0	-69.9	2.86 (2.97)	-	1.0	-	1.0	150 ± 20	>100
2	**4**	++	-92.1	-79.9	-69.5	2.85 (2.87)	2.2	1.1	0.7	1.0	27 ± 1	17 ± 2
3	**5**	+++	-136.4	-123.1	-110.9	2.70 (2.86)	2.4	1.1	0.8	1.0	37 ± 2	10 ± 1
4	**6**	++++	-142.7	-129.8	-110.1	2.63 (2.79)	2.1	1.5	6.0	1.0	0.33 ± 0.03[k]	>100
5	**7**		-188.8	-173.7	-143.6	2.50 (2.74)						
6	**2**						1.8	1.4	2.8	1.0	22 ± 2	95 ± 8
7	**8**	+++	-121.0	-104.6	-95.4	3.02 (2.93)[l]	-	1.2	0.7	1.0	110 ± 20	-
8	**9**						1.6	1.0	0.8	1.0	32 ± 1	8.0 ± 0.7
9	**10**						9.0	1.3	0.4	1.3	7.8 ± 0.7	4.5 ± 0.1
10	**11**						1.1	1.1	1.0	1.0	8.7 ± 1.4	8.2 ± 0.2

[a]Relative selectivity sequence for chloride binding from tandem MS experiments with mass-selected heterodimer/Cl^- complexes, see Fig. 3 for original data. [b]Interaction energy in monomeric NDI anion complexes computed with PBE1PBE/6-311++G**//PBE1PBE/6-311G** method and BSSE correction, see Fig. 4 for structures of **6**. [c]Equilibrium distance between chloride (nitrate) and NDI plane in monomeric complexes. [d-h]Relative NDI activity in EYPC-LUVs obtained in the HPTS assay with different extravesicular ions, *i.e.*, [d]external chloride (NaCl) compared to external iodide (NaI), [e]external chloride (NaCl) compared to external bromide (NaBr), [f]external nitrate ($NaNO_3$) compared to external acetate (NaOAc), and [g]external sodium (NaCl) compared to external potassium (KCl, 100 mM MX, all at constant 100 mM internal NaCl), see Fig. 5 and figs. S11, S14-S24. [h]Effective NDI concentration needed to reach 50% activity in the HPTS assay, data from Hill analysis of dose response curves (fig. S11). [i]Same for the CF assay (fig. S12). [j]See Fig. 1. [k]Lucigenin assay: $EC_{50} = 0.75 \pm 0.01$ μM (fig. S13). [l]Average distance from the two NDI planes of cyclophane **8**.

these promises could not be confirmed because the synthesis of tetracyano NDI **7** was unsuccessful.

Anion Transport. The transport activity of NDIs **2**-**11** was determined in large unilamellar vesicles composed of egg yolk phosphatidylcholine (EYPC LUVs) using different fluorescent probes[26]. In the HPTS assay, the vesicles loaded with the pH-sensitive fluorophore 8-hydroxy-1,3,6-pyrenetrisulfonate (HPTS) are exposed to a transmembrane pH gradient[13,14,20,26]. The dissipation of this pH gradient reported by EYPC-LUVs⊃HPTS can be attributed to H^+/M^+ antiport, OH^-/A^- antiport, H^+/A^- symport, OH^-/M^+ symport, HPTS efflux or vesicle destruction. In the CF assay, the vesicles are loaded with 5(6)-carboxyfluorescein (CF) at concentrations high enough to assure self-quenching[26]. EYPC-LUVs⊃CF report CF efflux or vesicle destruction as fluorescence recovery. In the LG assay, the vesicles loaded with the chloride-sensitive fluorophore lucigenin (LG) in nitrate buffer are exposed to external chloride[34]. EYPC-LUVs⊃LG selectively report chloride influx or vesicle destruction as fluorescence quenching.

Results from HPTS, CF and LG assays are quantified with EC_{50} and Hill coefficients n, which are both obtained from dose response curves[13,20,26]. The EC_{50} is the "effective" monomer concentration needed to reach 50% activity. EC_{50}'s are always overestimates because delivery, partitioning, self-organization and self-assembly are never quantitative. EC_{50} (HPTS) < EC_{50} (CF) demonstrates that ion transport is more efficient than dye export or vesicle destruction, EC_{50} (HPTS) < EC_{50} (LG, CF) can support cation selectivity, EC_{50} (HPTS, LG) < EC_{50} (CF) chloride selectivity, and so on.

NDI **3** was essentially inactive in HPTS and CF assay, decrowded and π-acidified NDIs **4** and **5** were clearly more active (Table 1, entries 1-3, figs. S11-S12). Sensitivity toward external anion but not cation exchange implied anion-selective transport (Fig. 5a-b). The anion selectivity sequence of NDIs **4** and **5** showed increasing activity with increasing hydration energy (Fig. 5b, figs. S16-S17). This so-called anti-Hofmeister behavior can be interpreted as support for strong binding to the transporter to overcompensate the cost of at least partial dehydration[13,26], although other explanations are possible. These results were compatible with transmembrane dimers of single-leaflet NDI bundles as plausible active suprastructures (Fig. 1c), ordered enough to generate significant anion selectivity and dynamic enough to let CF pass as well.

Improving activity with decrowding in **4** and π-acidification in **5** suggested that the decrowded and π-acidic NDI **6** should be perfect. Because of this perspective, difficulties to synthesize **6** were tackled and overcome (Fig. 2). This effort was worthwhile since NDI **6** exhibited nanomolar activity in both HPTS and lucigenin assays (figs. S13, S18), whereas non-specific activity in the CF assay was not detectable (Table 1, entry 4). Cations remained uninvolved in the transport, Cl^-/Br^- discrimination improved to 1.5 without significant losses in Cl^-/I^- selectivity, and a spectacular NO_3^-/AcO^- selectivity of 6.0 appeared (Table 1, entry 4, Fig. 5c).

The sequence $NO_3^- > ClO_4^- > SO_4^{2-} > AcO^-$ (obtained from the difference to a nearly linear anti-Hofmeister $Cl^- > Br^- > I^-$ correlation, Fig. 5b) was compatible with operational π,π-interactions in π-anion-π complexes, selecting for planar oxyanions with many π-bonds and rejecting tetrahedral α-carbons (Fig. 5c). The emergence of nitrate selectivity together with CF exclusion suggested that high self-organization of the active suprastructure is essential for π,π-enhanced anion-π interactions to occur. This interpretation was supported by the poor sensitivity of $Cl^- > Br^- > I^-$ sequences of NDIs **4**-**6** to supramolecular organization (fluoride exclusion with NDI **6** was attributed to Meisenheimer complexes[27]). Moreover, stabilization of the active dimeric bundles by vertical crosslinking in O-NDI rod **2** resulted in an intermediate NO_3^-/AcO^- selectivity of 2.8 at intermediate EC_{50} (HPTS) < EC_{50} (CF) (Table 1, entry 6, Figs. 5d, 1a). Formal horizontal crosslinking with O-NDI cyclophane **8** caused the corresponding loss in activity (Table 1, entry 7, fig. S19, Fig. 1d). This result further demonstrated that NDIs do not act as anion carriers, a conclusion that was fully supported by inactivity in U-tube experiments.

The addition of negative charges in NDI **10** gave outstanding halide selectivity without oxyanion recognition or CF exclusion (Table 1, entry 9, Figs. 5e and 1d). This

suggested that charge repulsion at the termini would loosen the active suprastructure, minimize the π,π-enhanced anion-π interactions accounting for nitrate selectivity but provide the free access to anion-π binding sites on monomer surfaces accounting for chloride selectivity. The complementary addition of positive charges in NDI **11** deleted all meaningful selectivity (Table 1, entry 10, Fig. 5f). Selectivity inversion to a very weak Hofmeister series testified for destructive interference from non-specific anion binding to the ammonium cations.

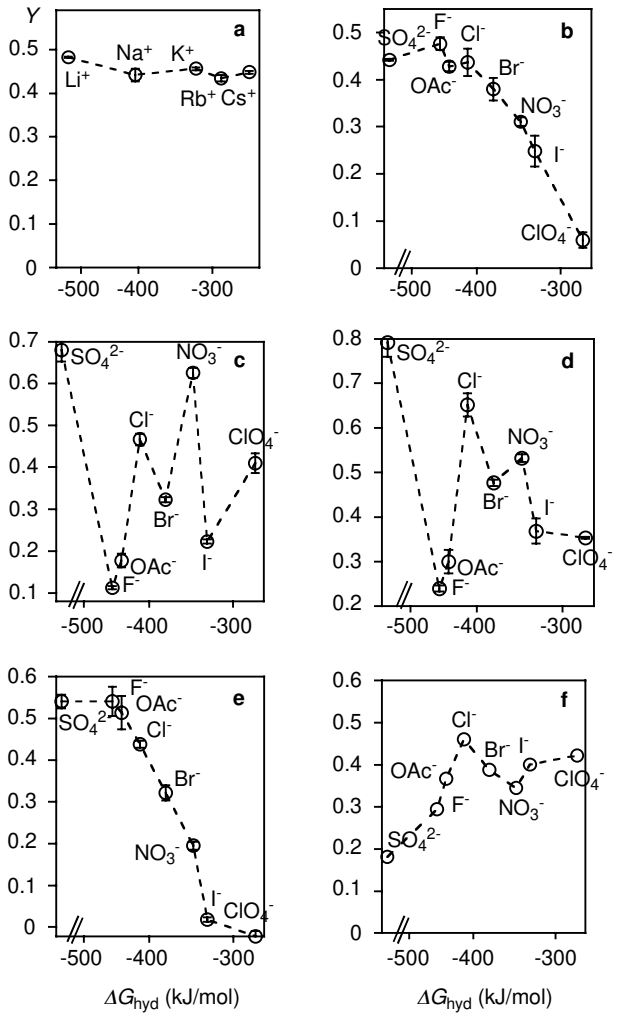

Figure 5 | Transport selectivity. Dependence of the fractional transport activity *Y* of NDIs **4** (**a**, **b**), **6** (**c**), **2** (**d**), **10** (**e**) and **11** (**f**) in the HPTS assay on the nature of extravesicular cations (**a**; 100 mM MCl, inside 100 mM NaCl) and anions (**b**-**f**; 100 mM NaX, inside 100 mM NaCl), see Supplementary Information for details.

Discussion

The objective of this study was to catch anion-π interactions at work. This evidence is secured from a collection of corroborative data on anion recognition and translocation from infrared multiphoton dissociation (IRMPD) MS-MS experiments, charge-transfer absorption, molecular modeling and transport in bilayer membranes. Ultimate evidence, as pure as possible, for the existence of anion-π interactions as such is obtained by IRMPD experiments with NDI models where only the π-acidic surface is left for anions to interact with (Fig. 3). To connect data from different methods, series of binding and selectivity sequences are recorded and compared. MS sequences demonstrate preferences for 1) chloride among halides, 2) nitrate among oxyanions, and 3) π-acidic, 4) decrowded and 5) dimeric binding sites. Molecular models confirm trends concerning π-acidity and active-site decrowding, models of 1:1 complexes the expected chloride > bromide > nitrate selectivity.

Comparison of binding with transport data reveals identical trends. π-Acidity and active-site decrowding are found to govern halide selectivity (Cl^- > Br^- > I^-), whereas supramolecular organization accounts for oxyanion selectivity (NO_3^- > ClO_4^- > SO_4^{2-} > AcO^- obtained from the difference to a nearly linear anti-Hofmeister Cl^- > Br^- > I^- background). This change occurs because the π,π-enhanced anion-π interactions thought to account for nitrate recognition are amplified in sandwich complexes, whereas normal anion-π interactions accounting for chloride recognition are not. Decreasing functional relevance with more easily oxidizable anions suggested that charge-transfer contributions to anion-π interactions are less relevant for function.

The perfect correspondence of transport data with affinity and selectivity sequences determined for anion-π interactions by tandem mass spectrometry and computational simulation demonstrates that anion-π interactions account for function. Particularly promising is the possibility to gain control of the nitrate recognition by π,π-enhanced anion-π interactions on the supramolecular level and chloride recognition by active-site engineering on the molecular level. Modular access to tuneable chloride, carbonate as well as nitrate sensors and transporters is of interest in biology and medicine. Channel replacement therapy has been proposed to rectify chloride channel malfunction in channelopathies such as cystic fibrosis[15-18], and carbonate transport and sensing is important in cellular respiration, cellular signaling, homeostasis and channelopathies[19]. The biological and therapeutic importance of nitrate and nitrite include cardiovascular diseases, global NO signalling, regulation of mitochondrial function, vasodilator action and tissue protection[34]. Nitrate, nitrite and NO research suffer from the unavailability of fluorescent nitrate/nitrite sensors that work in vivo[34]. π-π-Enhanced anion-π interactions combined with core-substituted NDI fluorophores of different color[35] offer an approach to the rational design of nitrate sensors. With regard to broader perspectives, our results on molecular recognition and translocation invite for a shift of attention toward molecular transformation. Complementary to the central importance of cation-π interactions in carbocation chemistry[12], anion-π interactions have the potential to catalyze enolate chemistry in a similarly fundamental manner.

Methods

The (tandem) mass spectrometric experiments described herein were conducted with an Ionspec QFT-7 FT-ICR mass spectrometer (Varian Inc., Lake Forest, CA), equipped with a 7 T superconducting magnet and a Micromass Z-Spray electrospray ionization (ESI) source (Waters Co., Saint-Quentin, France). The samples were introduced into the source as 50 μM solutions of NDI and the tetrabutyl ammonium salt of the corresponding anion in acetonitrile at flow rates of 1-2 μl/min. A constant spray and highest intensities were achieved with a capillary voltage of 3000-3800 V (depending on the used NDI and anion) and at a source temperature of 40 °C. The parameters for sample cone (20-45 V) and extractor cone voltage (8-10 V) were optimized for maximum intensities of the desired complexes. Multiple scans (20-50) were recorded and averaged for each spectrum in order to improve the

signal-to-noise ratio. After accumulation and transfer into the instrument's FTICR analyzer cell, the ions were detected by a standard excitation and detection sequence. For the fragmentation experiments, the ions of interest were mass selected in the ICR cell and irradiated with a 25 W CO_2 laser in the IR region [infrared multiphoton dissociation (IRMPD), 10.6 μm wavelength] to induce fragmentation.

Selectivity sequences for anion transport were determined with the HPTS assay[26]. In brief, 25 μl EYPC-LUVs⊃HPTS were added to 1950 μl gently stirred, thermostated buffer (10 mM Hepes, 100 mM 100 mM MCl ($M^+ = Li^+, Na^+, K^+, Rb^+, Cs^+$) or 100 mM NaX ($X^- = F^-, SO_4^{2-}$ (66 mM), $OAc^-, Cl^-, NO_3^-, Br^-, I^-, SCN^-, ClO_4^-$), pH 7.0) in a disposable plastic cuvette. The time-dependent change in fluorescence intensity (λ_{em} = 510 nm) was monitored ratiometrically (λ_{ex} = 450 nm, λ_{ex} = 405 nm) during the addition of base (20 μl 0.5 M NaOH), NDI (various concentrations in various solvents)[27], and gramicidin A (100 μM, 20 μl DMSO) for calibration. Fluorescence kinetics were normalized to fractional activities *Y* and plotted against hydration energies or as dose response corves for Hill analysis to extract EC_{50} and *n* (Tables 1 and S3).

Full experimental details on synthesis, MS-MS anion binding studies, charge-transfer absorption, molecular modeling and HPTS, CF, and LG transport assays can be found in the Supplementary Information[27].

References

1. Schottel, B. L., Chifotides, H. T. & Dunbar, K. R. Anion-π interactions. *Chem. Soc. Rev.* **37**, 68-83 (2008).
2. Gamez, P., Mooibroek, T. J., Teat, J. S & Reedijk, J. Anion binding involving π-acidic heteroaromatic rings. *Acc. Chem. Res.* **40**, 435-444 (2007).
3. Quinonero, D. *et al.* Anion-π interactions: Do they exist? *Angew. Chem. Int. Ed.* **41**, 3389-3392 (2002).
4. Mascal, M., Armstrong, A. & Bartberger, M. D. Anion-aromatic bonding: A case for anion recognition by π-acidic rings. *J. Am. Chem. Soc.* **124**, 6274-6276 (2002).
5. Alkorta, I., Rozas, I. & Elguero, J. Interaction of anions with perfluoro aromatic compounds. *J. Am. Chem. Soc.* **124**, 8593-8598 (2002).
6. Rosokha, Y. S., Lindeman, S. V., Rosokha, S. V. & Kochi, J. K. Halide recognition through diagnostic anion-π interactions: Molecular complexes of Cl^-, Br^-, and I^- with olefinic and aromatic receptors. *Angew. Chem. Int. Ed.* **43**, 4650-4652 (2004).
7. Gil-Ramírez, G., Escudero-Adán, E. C., Benet-Buchholz, J. & Ballester, P. Quantitative evaluation of anion-π interactions in solution. *Angew. Chem. Int. Ed.* **47**, 4114-4118 (2008).
8. Zaccheddu, M., Filippi C. & Buda, F. Anion-π and π-π cooperative interactions regulating the self-assembly of nitrate-triazine-triazine complexes. *J. Phys. Chem. A* **112**, 1627-1632 (2008).
9. Berryman, O. B., Bryantsev, V. S., Stay, D. P., Johnson, D. W. & Hay, B. P. Structural criteria for the design of anion receptors: The interaction of halides with electron-deficient arenes. *J. Am. Chem. Soc.* **129**, 48-58 (2007).
10. Hay, B. P. & Bryantsev, V. S. Anion-arene adducts: C-H hydrogen bonding, anion-π interaction, and carbon bonding motifs. *Chem. Commun.* 2417-2428 (2008).
11. Hay, B. P. & Custelcean, R. Anion-π interactions in crystal structures: Commonplace or extraordinary? *Cryst. Growth Design* **9**, 2539-2545 (2009).
12. Ma, J. C. & Dougherty, D. A. The cation-π interaction. *Chem. Rev.* **97**, 1303-1324 (1997).
13. Mareda, J. & Matile, S. Anion-π slides for transmembrane transport. *Chem. Eur. J.* **15**, 28-37 (2009).
14. Gorteau, V., Bollot, G., Mareda, J. & Matile, S. Rigid-rod anion-π slides for multiion hopping across lipid bilayers. *Org. Biomol. Chem.* **5**, 3000-3012 (2007).
15. Davis, A. P., Sheppard, D. N. & Smith, B. D. Development of synthetic membrane transporters for anions. *Chem. Soc. Rev.* **36**, 348-357 (2007).
16. Gokel, G. W. & Barkey, N. Transport of chloride ion through phospholipid bilayers mediated by synthetic ionophores. *New J. Chem.* **33**, 947-963 (2009).
17. Li, X., Shen, B., Yao, X. Q. & Yang D. Synthetic chloride channel regulates cell membrane potentials and voltage-gated calcium channels. *J. Am. Chem. Soc.* **131**, 13676-13680 (2009).
18. Deng, G., Dewa, T. & Regen, S. L. A synthetic ionophore that recognizes negatively charged phospholipid membranes. *J. Am. Chem. Soc.* **118**, 8975-8976 (1996).
19. Davis, J. T. *et al.* Using "small" molecules to facilitate exchange of bicarbonate and chloride anions across liposomal membranes. *Nature Chem.* **1**, 138-144 (2009).
20. Hennig, A., Fischer, L., Guichard, G. & Matile, S. Anion-macrodipole interactions: self-assembling, macrocyclic oligourea/amide anion transporters that respond to membrane polarization. *J. Am. Chem. Soc.* **131**, 16889-16895 (2009).
21. Bhosale, S. V., Jani, C. H. & Langford, S. J. Chemistry of naphthalene diimides. *Chem. Soc. Rev.* **37**, 331-342 (2008).
22. Jones, R. A., Facchetti, A., Wasielewski, M. R. & Marks, T. J. Tuning orbital energetics in arylene diimide semiconductors. Materials design for ambient stability of n-type charge transport. *J. Am. Chem. Soc.* **129**, 15259-15278 (2007).
23. Bhosale, S. *et al.* Photoproduction of proton gradients with π-stacked fluorophore scaffolds in lipid bilayers. *Science* **313**, 84-86 (2006).
24. Gabutti, S. *et al.* A rigid sublimable naphthalenediimide cyclophane as model compound for UHV STM experiments. *Chem. Commun.* 2370-2372 (2008).
25. Könemann, M. Naphthalenetetracarboxylic acid derivatives and their use as semiconductors. WO/2007/074137.
26. Matile, S. & Sakai, N. The characterization of synthetic ion channels and pores. In *Analytical Methods in Supramolecular Chemistry*, Schalley, C. A., Ed.; Wiley, Weinheim, **2007**, 391-418.
27. See Supplementary Information on *Nature Chemistry* Online.
28. Kogej, M. & Schalley, C. A. Mass spectrometry and gas phase chemistry of supramolecules. In *Analytical Methods in Supramolecular Chemistry*, Schalley, C. A., Ed.; Wiley, Weinheim, **2007**, 104-162.
29. Cooks, R. G., Patrick, J. S., Kotiaho, T. & McLuckey, S. A. Thermochemical determinations by the kinetic method. *Mass Spectrom. Rev.* **13**, 287-339 (1994).
30. Perdew, J. P., Burke, K. & Ernzerhof, M. Generalized gradient approximation made simple. *Phys. Rev. Lett.* **77**, 3865-3868 (1996).
31. Ernzerhof, M. & Scuseria, G. E. Assessment of the Perdew-Burke-Ernzenhof exchange-correlation functional. *J. Chem. Phys.* **110**, 5029-5036 (1999).
32. Frisch, M. J. *et al. Gaussian 03, Revision C.02,* Gaussian, Inc., Wallingford CT, **2004**.
33. McNally, B. A., Koulov, A. V., Smith, B. D., Joos, J.-B. & Davis, A. P. *Chem. Commun.* 1087-1089 (2005).
34. Butler, A. R. & Feelisch, M. Therapeutic uses of inorganic nitrite and nitrate - from the past to the future. *Circulation* **117**, 2151-2159 (2008).

35. Kishore, R. S. K. *et al.* Ordered and oriented supramolecular *n*/*p*-heterojunction surface architectures: Completion of the primary color collection. *J. Am. Chem. Soc.* **131**, 11106-11116 (2009).

Acknowledgments

We thank D.-H. Tran, J. Praz and L. Maffiolo for contributions to synthesis, D. Jeannerat, A. Pinto and S. Grass for NMR measurements, P. Perrottet, N. Oudry and G. Hopfgartner for MS, three anonymous reviewers for helpful suggestions, the Swiss National Supercomputing Center (CSCS) in Manno for CPU time, and the University of Geneva (S.M., J.M.), the University of Basel (M.M.), the Deutsche Forschungsgemeinschaft (C.A.S.), the Fonds der Chemischen Industrie (C.A.S.), the NCCR Nanoscale Sciences of the SNF (S.G., M.M.) and the Swiss NSF (S.M., M.M.) for financial support.

Author Contributions

R.E.D., V.R., J.M., T.T., S.G. and A.H. synthesized compounds, A.H. and R.E.D. transported ions across membranes, D.P.W. performed the (tandem) mass spectrometric experiments and evaluated the MS data, D.E. prepared computational models, M.M., J.M., C.A.S. and S.M. directed the study, contributing to design, execution and interpretation of experiments, to computer modeling and to manuscript writing.

Additional Information

Supplementary information accompanies this paper at www.nature.com/naturechemistry. Reprints and permission information is available online at http://npg.nature.com/reprintsandpermissions/. Correspondence and requests for materials should be addressed to S.M.

TOC graphic

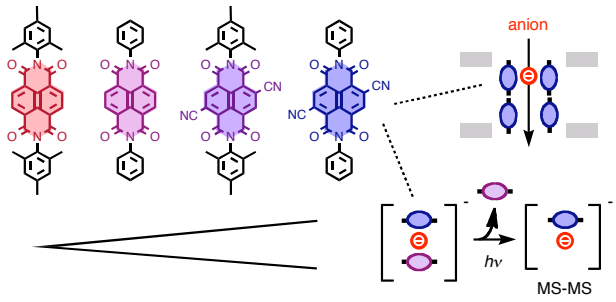

TOC text

For quadrupole moments up to +39 Buckinghams, increasing π-acidity of aromatic surfaces is shown to cause tighter anion binding in tandem mass spectrometry experiments, higher binding energies in molecular models, stronger charge-transfer absorption bands, and increasingly effective and selective anion transport across lipid bilayer membranes.